

GODDARD-GRANT

31P.

Princeton University Observatory  
Princeton, New Jersey 08544

1N-16762

FINAL REPORT  
Evaluation of Selected Detector Arrays for Space Applications

NASA Grant NAG5-241  
June 1, 1982 - June 30, 1985

Prepared for

National Aeronautics and Space Administration  
Goddard Space Flight Center  
Greenbelt, Maryland 20771

(NASA-CR-176979) EVALUATION OF SELECTED DETECTOR ARRAYS FOR SPACE APPLICATIONS Final Report, 1 Jun. 1982 - 30 Jun. 1985 (Princeton Univ. Observatory) 31 p CSCI 14B	N86-30124  Unclas G3/35 43241
--	--

Prepared by John L. Lowrance

August 7, 1986

## FINAL REPORT

NASA Grant NAG5-241

### Evaluation of IR-CCDs for Space Applications

This grant was in support of NASA's development of high density Schottky barrier IRCCD type image sensors for earth observations. Goddard Space Flight Center had a contract (NAS5-27800) with RCA Advanced Technology Laboratories to develop a dual band 512 pixel linear array capable of being butted end to end to make an arbitrarily long linear array.

The sensors were fabricated by RCA Laboratories, Princeton, New Jersey. This particular grant was to provide an independent assessment of the performance of the sensors. Progress on this task was dependent on the progress in fabricating the image sensors and this turned out to be slower than planned.

Appendix A summarizes measurements made on Palladium Silicide IRCCDs that were two-dimensional  $63 \times 32$  pixel arrays used by RCA to perfect their process for Palladium Silicide Schottky barrier technology.

Appendix B summarizes the test data on a 512 pixel linear array obtained late in the program but it does not necessarily represent the performance of the best devices made under the RCA contract.

The grant period of 9 months was extended to several years in waiting for sensors that were representative. The \$50,000 budget was conserved as much as possible but in the end there was insufficient funds to do the indepth testing of several devices contemplated initially.

The large package size for the 512 pixel linear array CCD was unexpected and required making a special dewar. This further eroded the funds available for testing. Figure 1 shows the complete assembly with the dewar and CCD facing down. The optical image from the lens is focused by a bellows onto the

CCD via a  $45^\circ$  mirror. Figure 2 is a view of the bottom of the dewar showing the CCD socket mounted on a printed circuit board that served to connect the CCD to the external electrical connectors. The CCD head electronics are in the chassis to the left. Present plans are to change the CCD socket so that the dewar can be used to test the new Tektronix 2048 x 2048 pixel CCDs.

## Figure Captions

Figure 1.  $\text{LN}_2$  dewar and optical assembly for testing 512 pixel IRCCD array.

Figure 2. View of dewar cold plate showing CCD socket assembly.

ORIGINAL PAGE IS  
OF POOR QUALITY

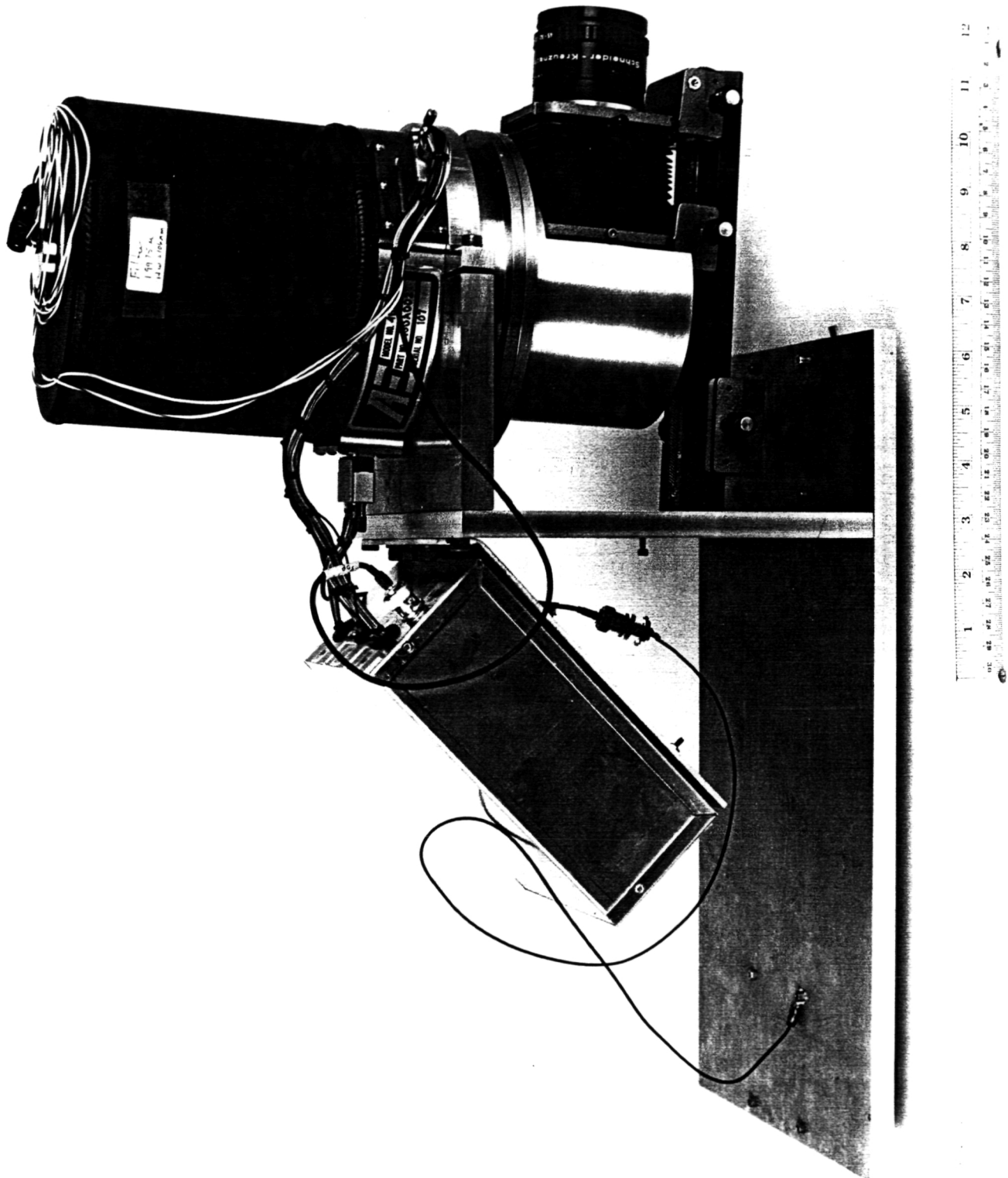


Figure 1

ORIGINAL PAGE IS  
OF POOR QUALITY

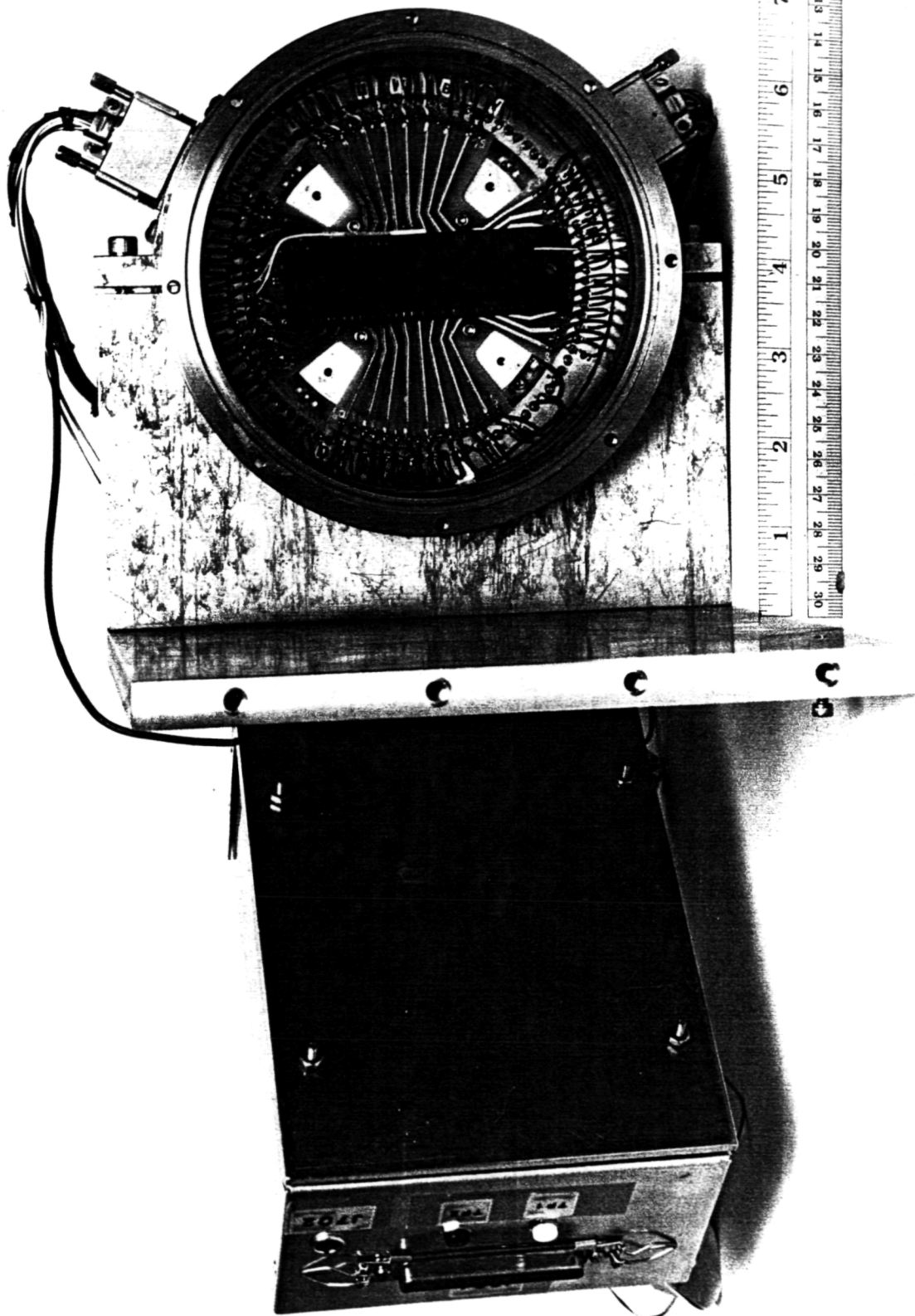


Figure 2

## APPENDIX A

CTE Measurements  
of an RCA  
Palladium Silicide IRCCD

Michael Reale and  
Paul Zucchino  
Princeton University  
March 1983



### Table of Contents

1.0	Introduction
2.0	General Characteristics
3.0	CTE versus Uniform Exposure
4.0	Serial CTE versus Temperature
5.0	Comparison of Electrical & Optical Fat Zeros
6.0	Parallel CTE

## 1.0 INTRODUCTION:

We have conducted a limited series of laboratory measurements of the characteristics of one Palladium Silicide Infrared Charge Coupled Device (IRCCD) fabricated by RCA, Serial number 11G-77. The laboratory work was focused on the CTE (Charge Transfer Efficiency) and other related parameters of the device. We wish to emphasize that the work was limited to one device, and might be compromised by our lack of experience with this particular type of CCD.

## 2.0 GENERAL CHARACTERISTICS:

Figure 2.1 shows the organization of the photosites, lines, and pixels at the IRCCD. This IRCCD has 63 lines of 32 pixels each for a total of 2016 IR photosites. The connection between the parallel transfer area (the B register) and the serial output register (the C register) is configured so that the signal charge packets from the 32 photosites per line are transferred into alternate pixels of the C register; that is, there are 64 active pixels in the C register, 32 are loaded with the signal charge packets transferred from the B register, and the other interleaved 32 pixels receive no charge during B to C transfers.

We call the interleaved pixels which are not loaded with signal charge the "null" pixels. We intentionally clock the C register and the output amplifier elements so that each of the 64 active pixels is readout as an individual pixel. This yields a serrated video output signal with each real image pixel being followed by a null pixel. Any charge that is seen in the null pixels (excluding any electrical fat zero that may have been introduced

at the beginning of the C register) is the result of charge transfer inefficiency in the C register. The effect of charge transfer inefficiency is to smear charge from the pixels that are carrying charge into trailing pixels.

The test conditions were:

Frame period: 9.6 milliseconds.

Pixel period: 2.0 microseconds.

Temperature 93K° unless otherwise noted.

Optical input wavelength range: 1.26 - 2.12 microns.

Setup voltages:

1/3CHI	†06.85	1/3CLO	-11.67	2/4CHI	†07.70	2/4CLO	-09.31
G6CHI	†19.08	G6CLO	†00.53	G3CHI	-20.18	G3CLO	-19.87
G2C	†21.85	G4C	+04.03	G5C	+09.00	VGG	†02.01
VD	†19.87	VDD	†19.97	VSHI	†19.88	VSLO	+19.92
1/3BHI	†04.63	1/3BLO	-13.38	2/4BHI	†08.84	2/4BLO	-08.00
VTHI	†16.80	VTLO	-00.49	G1HI	-00.32	G1LO	-00.40
1/3AHI	-10.80	1/3ALO	-11.71	2/4AHI	-03.79	2/4ALO	-03.70
G3AHI	-17.47	G3ALO	-17.46	G2A	-00.24		

Observed charge capacities:

(Me/pixel = Million electrons per pixel)

C register: 1.8 Me/pixel (above this level CTE rapidly degraded; actual C register spillover was above 7 Me/pixel.)

B register: 3.7 Me/pixel (spillover).

Output stage: 5.2 Me/pixel (saturation).

Output stage charge sensitivity: 0.82 MV/electron.

### 3.0 CTE VERSUS UNIFORM EXPOSURE

An earlier series of measurements on this device was intended to explore its photometric linearity. This was done because qualitative laboratory work had indicated an apparent loss of sensitivity at low exposure levels. We now

believe that there is no true loss in sensitivity, only a degradation in CTE at small signal levels. At the time of the linearity tests the null pixels were not being readout, only the signals generated by the charge in the active pixels were processed, displayed and digitized. The device was exposed to uniform illumination at various levels. The video generated at various pixel locations was compared to the illumination-induced portion of the device's reset current, that is, the IRCCD was being used as its own average exposure meter by monitoring the reset current. For exposures above 400 ke/pixel (ke = 1000 electrons) the output signal versus exposure function was linear, but for lower exposures, especially below 50 ke/pixel, there was significant departure from linearity. Both the magnitude and sign of the non-linearity depended on where the pixel was in the frame.

At first we were surprised to see what was suspected to be a CTE effect with a uniformly illuminated frame. We had expected that any CTE effects would be self cancelling in that any charge smeared from one pixel to a following pixel would be balanced by the same amount of charge being smeared to yet the next pixel, etc. This simplistic model neglects the boundary (raster edge) effects that are not negated by uniformly illuminating the whole frame.

In this report the terms top, bottom, left, and right refer to the image of the array of photodiodes as it appears on a standard television display; the first pixels readout of the C register appear on the left of the display, and the first line of pixels transferred from the B register to the C register appears at the top of the display.

There are two reasons why CTE caused apparent photometric non-linearity in our tests. The first is there are no pixels below and to the right of those pixels in the lower right corner on successive frame readouts. Conversely the upper left corner pixels are pre-charged with the residual charge of all the pixels transferred through that corner in previous successive readouts of the uniformly illuminated frames. Consequently at low exposure levels where poor CTE is encountered, there is a general brightening of the upper left corner and a general relative dimming of the lower right corner, even if both the illumination and the photodiode sensitivities are uniform.

The second reason CTE affected our linearity results is that at first we were ignoring the charge in the null pixels which are interleaved between the active pixels in the C register as explained in Section 1.0, the Introduction. The first-order effect of poor CTE in the C register is to effectively transfer charge from each active pixel to the null pixel directly behind it in the C register. When this was understood, we arranged to readout the null pixels with the same video and data processing as the active pixels so that we could use the charge found in the null pixels as a C register CTE diagnostic tool.

To explore the effects of CTE with uniform illumination, the data of Figures 3.1 through 3.4 were gathered. Uniform illumination exposures ranging from 2.0 Me/pixel (Me - million electrons) down to 19 ke/pixel were made. Data from four active pixels near the corners of the frame, and from their respective trailing null pixels, were recorded. The following table correlates the figures with the positions of the data pixels in the frame:

FIGURE	LOCATION	LINE (of 63)	PIXEL (of 32 active)
3.1	Upper Left	5	4
3.2	Upper Right	5	29
3.3	Lower Left	61	4
3.4	Lower Right	61	29

On each figure both the active pixel signal output and the trailing null pixel signal output are plotted. Note that the signal scale for the active pixels are tenfold the signal scale for the null pixels. Accordingly the point of intersection of the two curves in each figure gives the exposure level at which the null pixel signal is 10% of the active pixel signal.

Comparing Upper Left (3.1) with the Upper Right (3.2) and comparing the Lower Left (3.3) with the Lower Right (3.4) reveals the effects of serial or C register CTE. Figure 3.2 shows that at exposures below approximately 200 ke/pixel, the fraction of the active pixel signal that appears in the trailing null pixel grows markedly. From this location, both the active and the null pixel signals have transversed about 90% of the C register's total length of 32 active pixels or 64 total pixels.

Another interesting effect seen in both Figures 3.2 and 3.4 is the sharp increase in null pixel signal with exposures above 1.0 Me/pixel. RCA attributes this effect to a transition from normal buried channel operation to a partial surface channel mode as the amount of charge in the C register well exceeds 1.0 Me/pixel. The characteristically poor CTE of surface channel operation causes the sharp increase in "left-behind" charge above 1.0 Me/pixel.

Figure 3.1 shows the left-behind charge which rises from 50% to 75% of the active pixel signal for exposures below 100 ke/pixel. Why does a null pixel which only followed its active pixel through 8 total pixel transfers show such a large signal? We believe this is because of all the previous charge packets that were transferred through this null pixel location in previous successive line line readouts. It seems that CCD's are replacing electron beam imagers so comprehensively that they even mimic "lag" at low signal levels! In applications where the timing constraints allow, overclocking or "overscanning" of the C register can be used to erase the residual charge to a large extent.

Parallel, (vertical) or B register CTE effects are decidedly less apparent in these four figures because, as discussed later in this report, the B register CTE is significantly better than that of the C register.

Comparing the Upper Figures: 3.1 & 3.2, against the Lower Figures: 2.3 & 2.4, respectively one can see the "brightening at the top" and "dimming at the bottom" effect of reduced CTE at exposures below 200 ke/pixel. This is best seen in the Right pair (Figures 3.2 & 3.4) since the effect is not masked by the C register lag discussed above.

#### 4.0 SERIAL CHARGE TRANSFER EFFICIENCY vs TEMPERATURE

In this experiment we wanted to observe the behavior of the IRCCD over a temperature range of 80 to 120°K. For application as a passively cooled camera, 120°K would be the nominal operating temperature.

For our laboratory tests the IRCCD is mounted in a liquid nitrogen cooled dewar. The usual operating temperature is near 77°K (the boiling point of liquid nitrogen). In order to reach 120°K we let the nitrogen boil away and the dewar slowly warm up. During this warming up period, pictures of the video waveforms were taken while the temperature and total photocurrent of the CCD were recorded.

An exposure level of 79 mV (96 ke/pix) was selected because at this level the response of the device was seriously compromised by SCTE (Serial Charge Transfer Efficiency) degradation. The exposure level was kept constant and the temperature allowed to increase.

There was no apparent change in SCTE as the device warmed up from 101°K to 126°K. At 131°K the SCTE began to improve. A crisp image appeared at 138°K. The image at 138°K is similar to operating at 101°K with 106 ke/pixel of optical fat zero. The characteristic smearing at low exposure levels due to charge transfer inefficiency is remedied by the "thermal fat zero" provided at 138°K. At 138°K the background is 10% of the dynamic range.

The graph (Fig. 3.1) depicts apparent SCTE vs temperature and apparent thermal fat zero vs temperature.

Apparent SCTE is an arbitrary value arrived at in the following manner:

$$ASCTE = \left( 1 - \frac{\text{Height of null pixel}}{\text{Height of active pixel} + \text{Null pixel}} \right) 100\%$$



Note: Heights are relative to baseline. The same null and active pixels are used each time. The 3 pixel wide test image was 20 active pixels into the image representing 40 serial transfers.

Another term requiring explanation is apparent thermal fat zero (ATFZ). ATFZ at higher temperatures is calculated as follows:

$$\text{ATFZ} = (\text{Detector photocurrent at the higher temperature}) \\ - (\text{Detector photocurrent at } 101\text{K})$$

The resulting difference is converted to ke/pixel.

Since exposure level is kept constant the increase in detector photocurrent as temperature increases is all thermally generated. Therefore the values we obtain for ATFZ are the increases in thermally generated current relative to 101°K. We do not need to know the absolute values since we wish only to observe the trend thermal fat zero follows as temperature increases.

It is clear from the graph (Fig. 3.1) that as the temperature increases both ATFZ and ASCTE increase exponentially.

At low exposure levels in order to have adequate CTE, this IRCCD requires either electrical or optical fat zero. We think the reason CTE improves with temperature is because thermally generated current is providing a form of fat zero. This increase in thermally generated current we call thermal fat zero.

It should be noted that our temperature readings are obtained by means of a silicon diode which is an integral part of the detector chip. This is an ideal location for the temperature sensor. When the dewar is completely filled with liquid nitrogen the temperature reading is about 15 to 20°K above the boiling point of nitrogen. Allowing for thermal drop between the coolant and the detector, we suspect that the sensor reading (based on 2.0 mV/°c) could be as much as 15°K higher than the actual temperature of the IRCCD.

## 5.0 COMPARISON OF ELECTRICAL AND OPTICAL FAT ZEROS

At the lowest distinguishable exposure levels serial charge transfer efficiency is at a minimum. As is well documented, crisp images are possible at low light levels by using optical fat zero (OFZ).

An alternative for increasing serial charge transfer efficiency (SCTE) is injection of electrical fat zero (EFZ) into the "C" register. Therefore we ran comparisons of EFZ to OFZ.

The "C" register is made up of alternate active and null pixels. OFZ only raises the dc level of the active pixels, whereas EFZ raises the DC level of both the active and the interleaved null pixels.

In our experiment we injected fat zero (optical or electrical) at low exposure levels until the SCTE was nearly 100%. SCTE was gauged by observing the trace signal from a line of pixels on an oscilloscope. When all the null pixels had the same zero signal baseline, charge spillage into the empty pixels was minimal. At this point SCTE was assumed to be nearly 100%. Comparison of video waveform pictures at equal exposure levels revealed that EFZ has a similar effect on upgrading SCTE as OFZ. What is not clear is why EFZ, which also fills the null pixels, was not more effective than OFZ in improving SCTE.

In addition to photographing oscilloscope traces we took electrometer readings of total detector current. Table 4.1 lists four exposure levels and the corresponding electrical or optical fat zeroes, in Kilo-Electrons/pixels necessary to bring SCTE up to nearly 100%.

TABLE 5.1

<u>Test Exposure</u>			<u>Optical fat zero</u>	<u>Electrical fat zero</u>
<u>mV</u>	<u>ke/pixel</u>	<u>ACTE</u>	<u>(ke/pixel)(32pixels/line)</u>	<u>(ke/pixel)(64pixels/line)</u>
210	256	72%	184	151
130	159	61%	133	119
79	96	52%	118	86
30	37	40%	102	116

The total detector current for EFZ was on the average 1.8 times greater than OFZ. This is as expected since EFZ injects charge into the null pixels also.

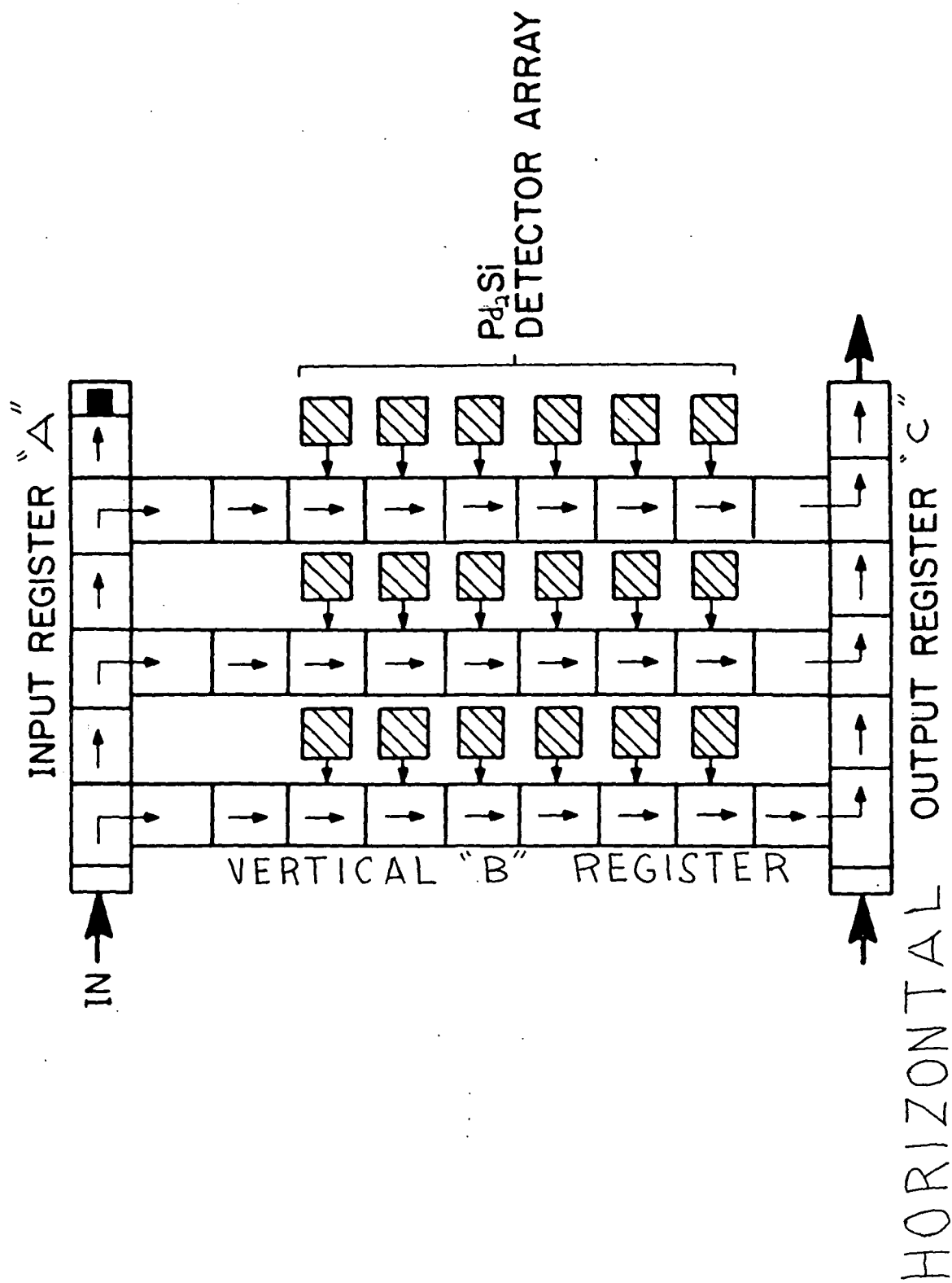
Electrical fat zero has two distinct disadvantages. First, it appeared that EFZ introduced more noise into the system since the oscilloscope traces were noticeably more noisy. The second disturbance occurred after the clocking patterns were changed so we would be able to inject EFZ into the C register. The effect of this change was brightening of the pixels on the extreme left hand side of the image. This bright edge obliterated any images in that portion of the CCD. This phenomena is not understood and may be unique to this device or clocking pattern to inject the electrical signal.

## 6.0 PARALLEL CHARGE TRANSFER EFFICIENCY

We were interested in determining the extent of parallel charge transfer efficiency (PCTE) degradation in the vertical "B" register. Earlier attempts at conducting this study were hampered by SCTE which degrades rapidly with decreasing exposure levels. In order to control and limit the SCTE degradation, EFZ was injected into the horizontal "C" register.

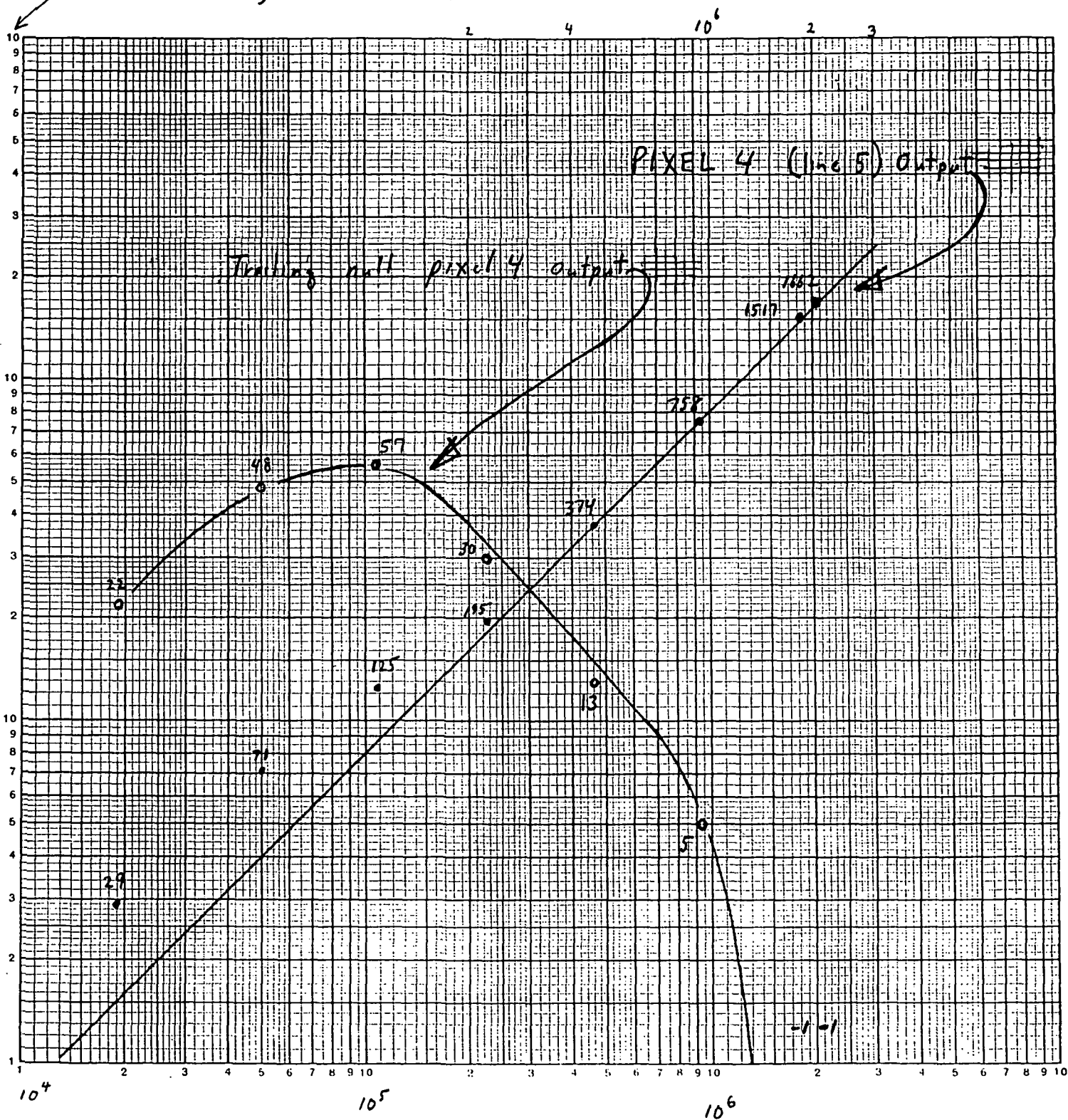
PCTE was gauged in a qualitative manner. We observed the envelopes of every horizontal line of pixels on the oscilloscope. The target was a wide slit 14 horizontal lines of pixels tall. Therefore at high exposure levels, where PCTE is not expected to be a problem, 14 envelopes will be clearly defined from their empty neighbors. At low exposure levels, should PCTE degradation occur, envelope distortion will occur at the leading and trailing edges of the slit.

We maintained adequate SCTE by injecting EFZ into the "C" register and were able to observe 14 equally tall and well shaped envelopes at the lowest exposure levels. We conclude that the PCTE is substantially better than the SCTE.



Upper Left Pixel Output and Trailing Null Pixel Output

vs Exposure (measured via reset current)

 $10^4$  for main pixel,  $10^3$  for trailing pixel

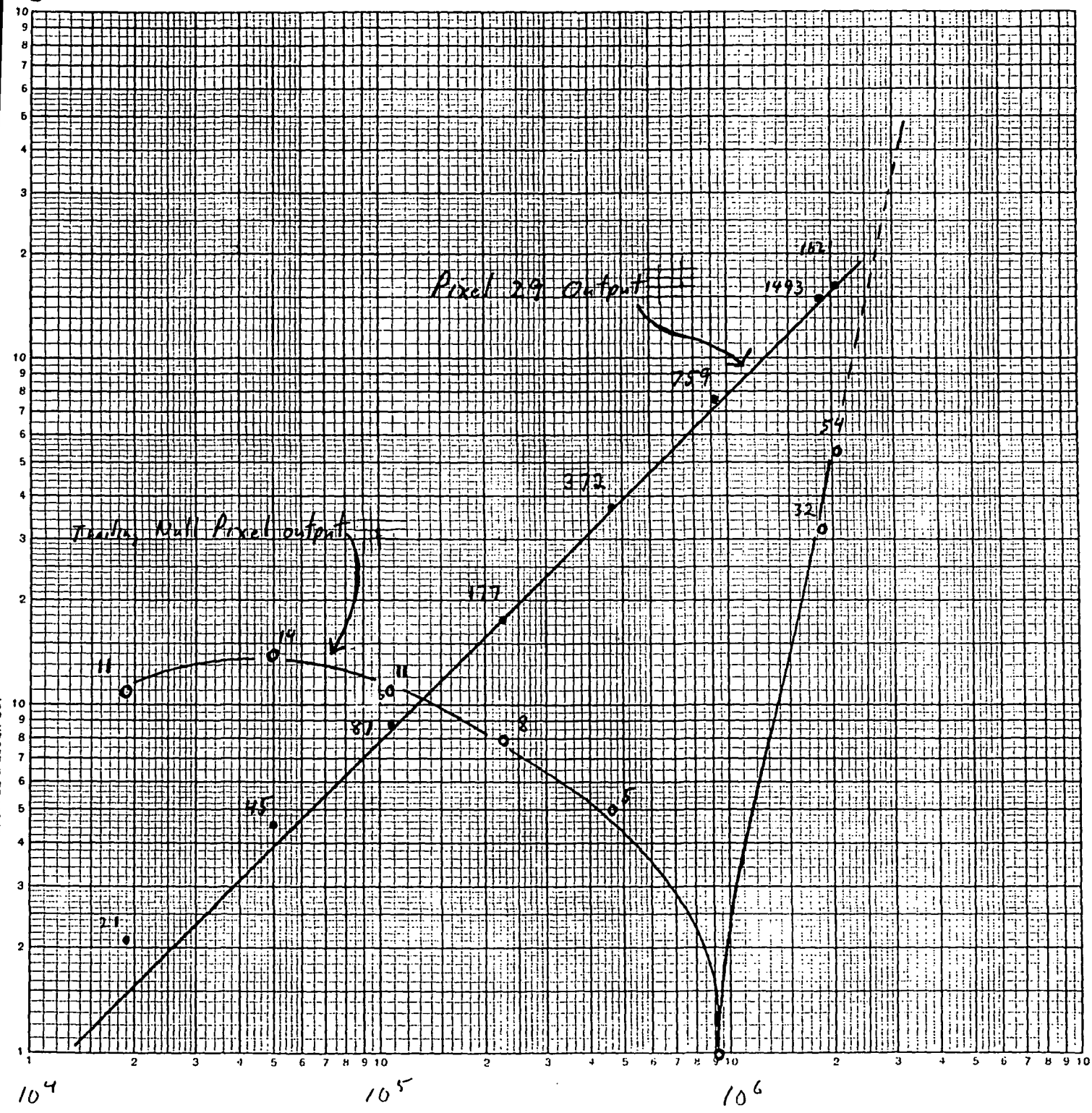
pe/pixel mean exposure (via reset current)

Figure 3.1

# Upper Right Pixel Output and Trailing Null Pixel Output

ORIGINAL PAGE IS  
OF POOR QUALITY

←  $10^4$  for main pixel,  $10^3$  for trailing pixel



pe/pixel

Figure 3.2

LL Line 01(0160) Pixel 1 (0162)

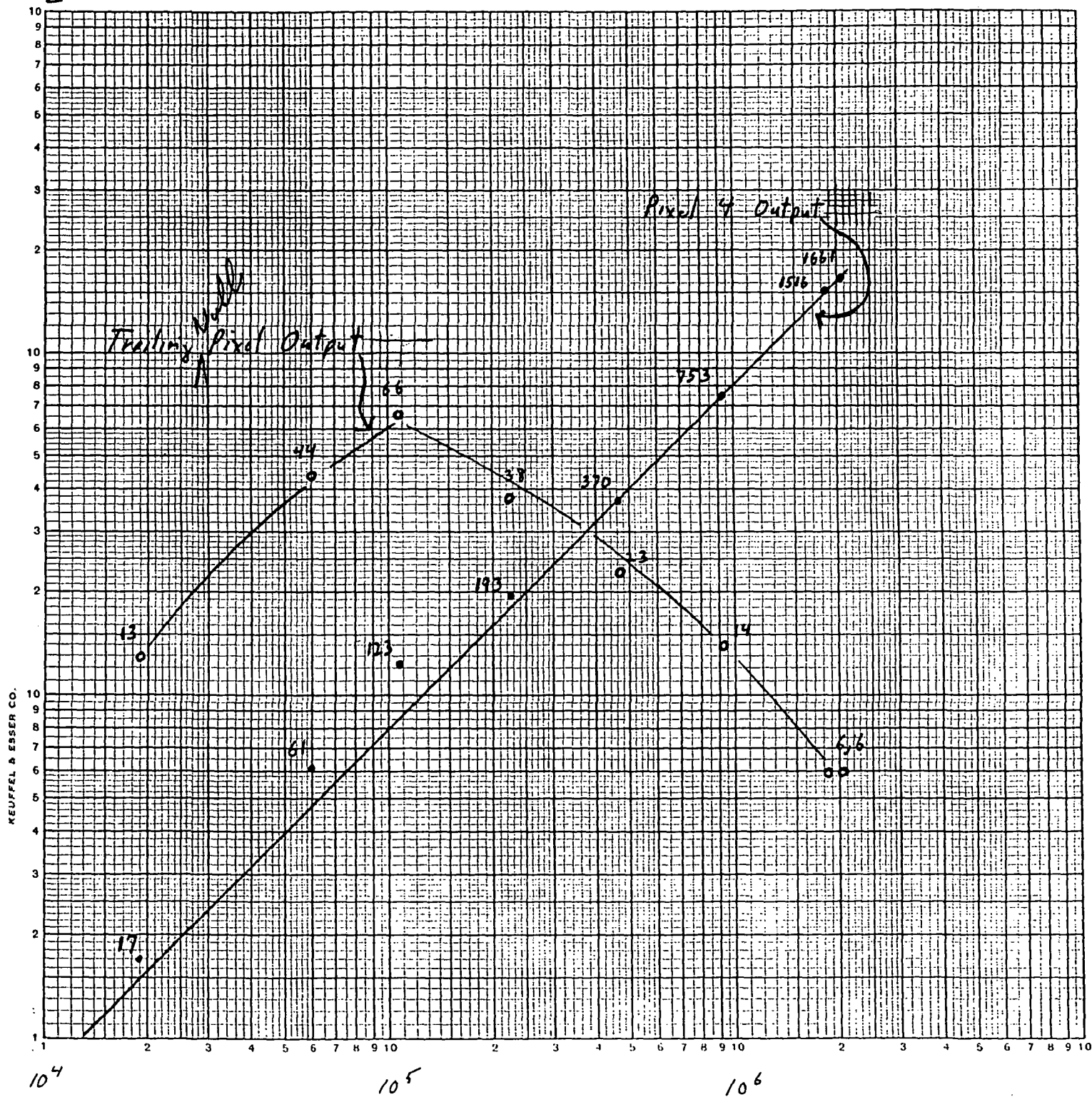
ORIGINAL PAGE IS  
OF POOR QUALITY

2-13-83

3-20-83

Lower Left Pixel Output and Trailing Null Pixel Output

$10^4$  for main pixel,  $10^3$  for trailing pixel



$p_e/\text{pixel}$

Figure 3.3



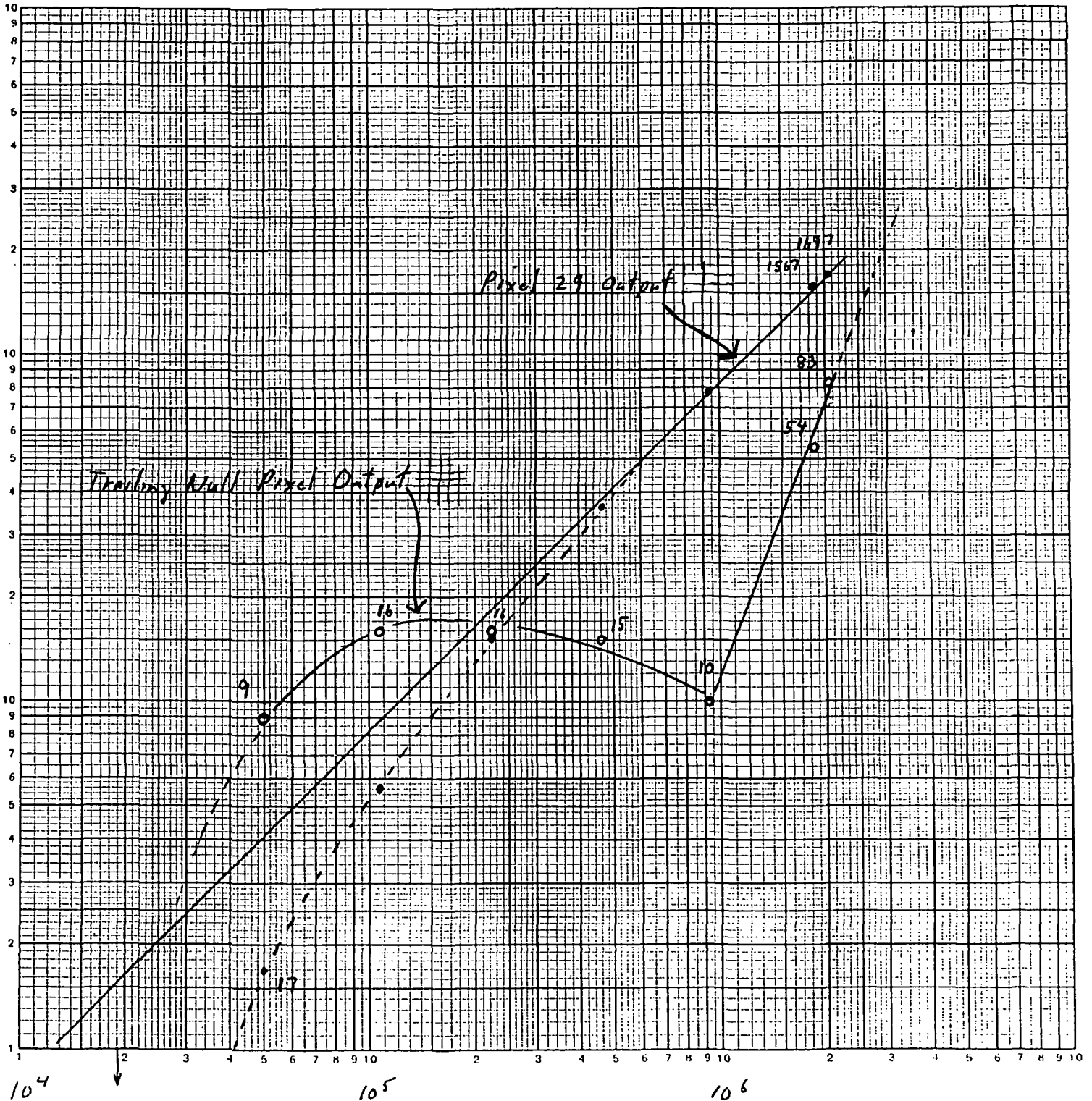
18

LK = Line 61 (of 63) Pixel 29 (of 32)

2-13-83

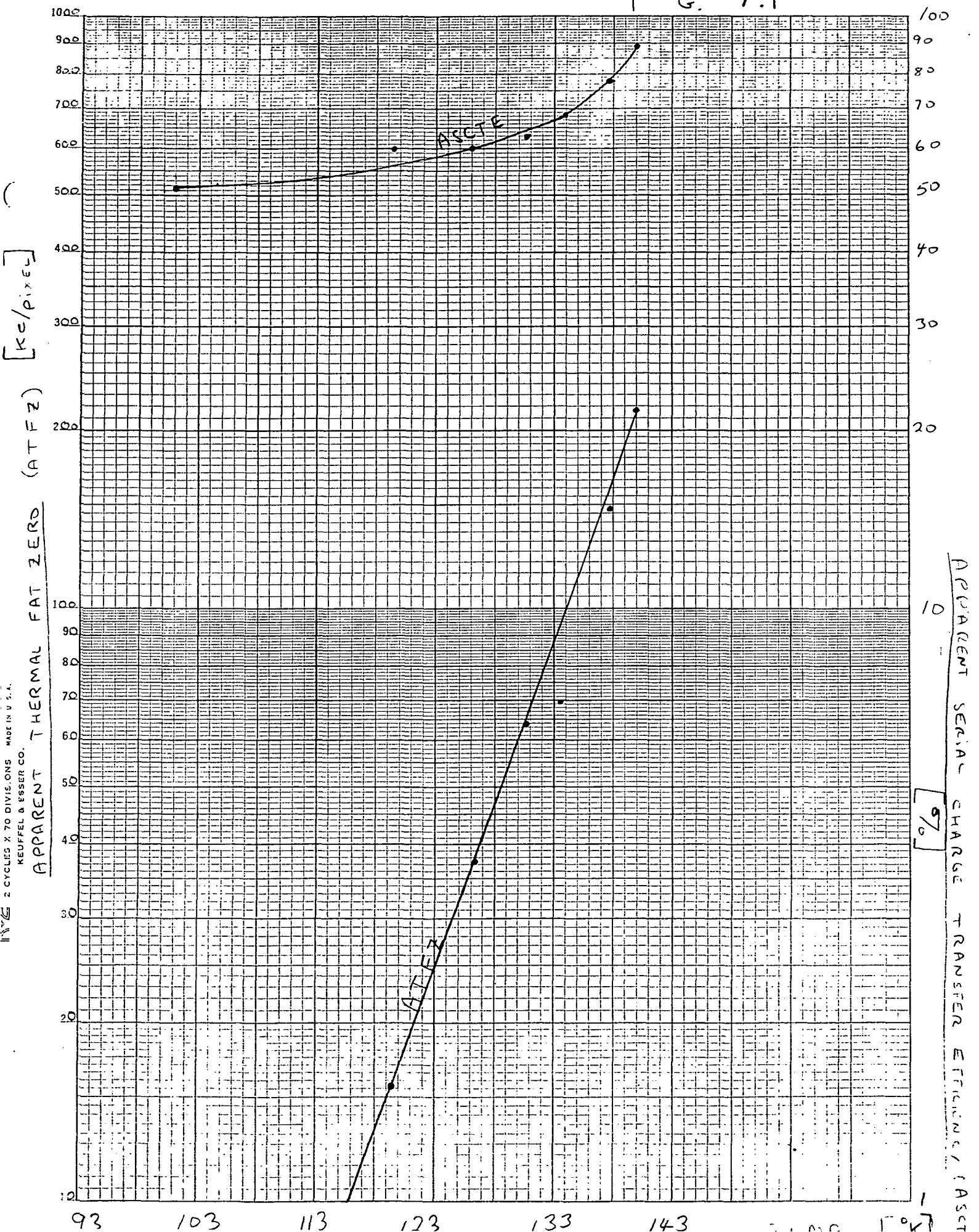
Lower Right Pixel Output and Trailing Null Pixel Output

$10^4$  for main pixel,  $10^3$  for trailing pixel



pe/pixel

Figure 3.4



## APPENDIX B

# Summary of Test Data for SWIR Detector Array

Serial Number - REV3, COL 9

Optical filter:  $\lambda_0 = 1.9975 \mu\text{m}$ ,  $\text{HW} = 106 \text{ nm}$

Pixel time:  $8 \mu\text{s}$

Full well =  $0.9 \times 10^6$  electrons\*

Noise = 97 electrons\*

\* Transfer response used was  $1.04 \text{ e}/\mu\text{V}$ , which was based on info on the RCA's "Operating Conditions" data sheet furnished with the array.

Single Pixel Response: (5000 e Electrical Flat Zero except where noted.)

80% FW  $\rightarrow$  40%

17% FW  $\rightarrow$  39%

8% FW  $\rightarrow$  36%

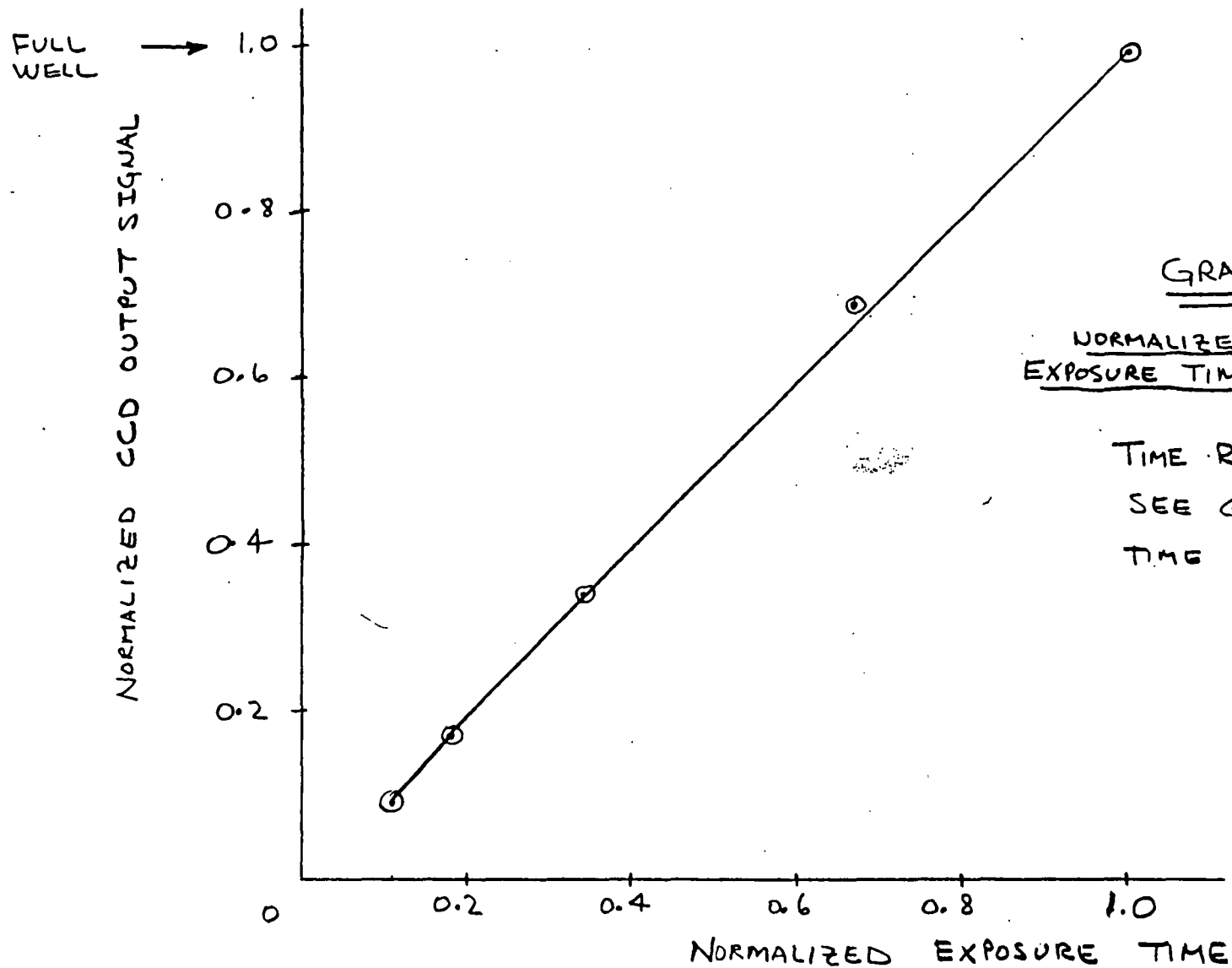
1% FW  $\rightarrow$  32%

1% FW without flat zero  $\rightarrow$  none

GRAPHS 1 & 2 show transfer response  
without Fat Zero and 5000 e  
Fat Zero at 2.8% of full well.

Dewar was cooled to  $-168^{\circ}\text{C}$

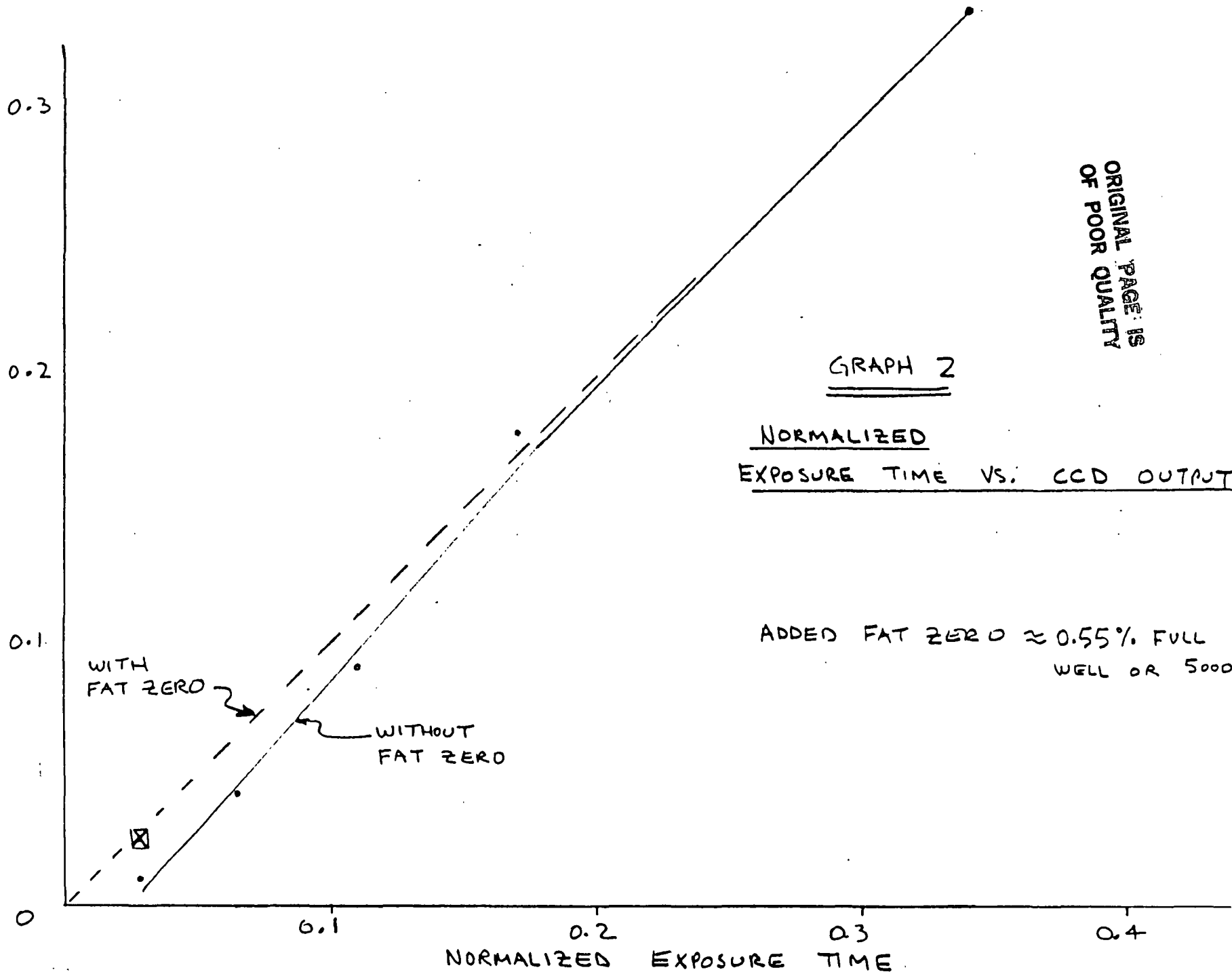
Dark Current  $\sim 1.8 \times 10^5 \text{ e/sec}$



GRAPH 1  
NORMALIZED  
EXPOSURE TIME VS. CCD OUTPUT

TIME RANGE 1.0 to 0.11,  
SEE GRAPH 2 FOR  
TIME RANGE 0.34 TO 0.028

NORMALIZED CCD OUTPUT SIGNAL (OF FULL WELL)



ORIGINAL PAGE IS  
OF POOR QUALITY